International Journal of Refrigeration 128 (2021) 287–298

Contents lists available at ScienceDirect

International Journal of Refrigeration

journal homepage: www.elsevier.com/locate/ijrefrig

Experimental evaluation of zeotropic refrigerants in a dedicated mechanical subcooling system in a CO_2 cycle

Rodrigo Llopis[a,*], Gabriele Toffoletti[b], Laura Nebot-Andrés[a], Giovanni Cortella[b]

[a] Thermal Engineering Group, Mechanical Engineering and Construction Department, Jaume I University, Spain
[b] Polytechnic Department of Engineering and Architecture, University of Udine, Italy

ARTICLE INFO

Article history:
Received 11 December 2020
Revised 22 April 2021
Accepted 19 May 2021
Available online 25 May 2021

Keywords:
CO_2
Mechanical subcooling
R-152a
Zeotropic
Refrigeration

ABSTRACT

Use of zeotropic blends in the dedicated mechanical subcooling system of a CO_2 refrigeration system was suggested as a possible improvement due to matching of evaporating temperature with CO_2 temperature profile during subcooling. This work has verified this possibility and has determined theoretically the best performing compositions of R-600, R-32 and CO_2 with the base fluid R-152a. Then, the mixtures have been tested experimentally in a lab-test bench for constant heat load temperature for three heat rejection temperatures (25.1, 30.3 and 35.1°C). Optimum conditions are measured (subcooling degree and heat rejection) and a COP increase of 1.4% has been obtained. The work, for the optimum conditions, analyses the operating parameters of the cycles and focus specially on the thermal parameters of the subcooler. It has been verified that the use of zeotropic mixtures allows to reduce irreversibilities in the cycle, as pointed out theoretically by Dai et al. (2018).

Évaluation expérimentale des frigorigènes zéotropes dans un système à sous-refroidissement mécanique dédié dans un cycle au CO_2

Mots-clés: CO_2; Sous-refroidissement mécanique; Zéotrope; Froid [artificiel]

1. Introduction

Subcooling has been recognised during the last years as a useful technology to enhance the performance of refrigeration cycles. Subcooling, as reviewed by Park et al. (2015) for subcritical cycles, consists in chilling the liquid at the exit of the condenser, thus incrementing the refrigerating effect and, in general, improving the coefficient of performance. However, when subcooling is used in transcritical systems the benefits of this method are taken to an extreme, as analysed by Llopis et al. (2018). In transcritical cycles the decoupling between pressure and temperature in the supercritical region makes it possible to reduce the enthalpy of the refrigerant at the inlet of the first expansion stage and at the same time to cut down the optimum heat rejection pressure. The combination of both outcomes increases the refrigerating effect and at the same time reduces the compression ratio and thus diminishes the power consumption of the compressor, resulting in large increments on capacity and COP. Specifically, using internal heat exchangers increments up to 12% in COP have been measured (Torrella et al., 2011), using economizers up to 21% (Cavallini et al., 2005) and using thermoelectric subcoolers up to 9.9% (Sánchez et al., 2020).

Concretely, one of the most appealing methods is the subcooling based on an external vapour compression cycle, known as dedicated mechanical subcooler (DMS) (Bertelsen and Haugsdal, 2015; Llopis et al., 2015). In this case the subcooling is provided at the exit of the condenser/gas-cooler using an auxiliary vapour compression cycle with a heat exchanger (subcooler) where a different refrigerant evaporates. The main characteristic of this system is that both cycles, the main and the auxiliary, perform heat

* Corresponding author.
E-mail address: rllopis@uji.es (R. Llopis).

https://doi.org/10.1016/j.ijrefrig.2021.05.028

Nomenclature

BP	Back pressure valve
COP	coefficient of performance
$\dot{E}_X$	exergy, kW
Glide	phase-change temperature difference at constant pressure, K
GWP	global warming potential at 100 years
h	specific enthalpy, kJ•kg^{-1}
h_{fg}	latent heat of phase-change, kJ•kg^{-1}
k	compression ratio
$\dot{m}$	refrigerant mass flow, kg•s^{-1}
M	molar mass, g•mol^{-1}
p	pressure, bar
P_C	compressor power consumption, kW
$\dot{Q}_o$	cooling capacity of the CO_2 cycle, kW
RU	superheating degree, K
s	specific entropy, kJ•kg^{-1}•K^{-1}
SUB	CO_2 subcooling degree in subcooler, K
t	temperature, °C
v	specific volume, m^3•kg^{-1}
V	volumetric flow rate, m^3•kg^{-1}
VCC	volumetric cooling capacity, kW•m^{-3}

Subscripts

base	refers to CO_2 cycle without subcooling
d	death state level
DMS	refers to the dedicated mechanical cycle
e	effective
CO2	refers to the CO_2 cycle
g	refers to glycol as secondary fluid in CO_2 evaporator
gc	gas-cooler
in	inlet
K	refers to condensing level
l	refers to saturated liquid
lmtd	logarithmic mean temperature difference
O	refers to the evaporating level
out	outlet
sub	subcooler
v	refers to saturated vapour
w	refers to water as secondary fluid for heat rejection

Greek symbols

η_G	compressor overall efficiency
ε	thermal effectiveness

rejection at the same temperature level. Initial experimental tests in single-stage plants measured capacity and COP improvements of 55.7% and 30.3% respectively using R-1234yf as refrigerant in the DMS (Llopis et al., 2016) only with the optimization of the heat rejection pressure. Later, with an updated version of the plant and using R-152a in the DMS (Nebot-Andrés et al., 2021), they demonstrated the existence of optimum working parameters and determined them, heat rejection pressure and subcooling degree, which are the two main variables to control in this cycle. In relation to the application of the DMS to CO_2 booster systems, authors have only found the experimental work of Bush et al. (2017), who tested a lab-scale plant with R-134a in the DMS, measuring a COP improvement of 9.5%. Nonetheless, the use of the DMS with booster systems has been analysed with different approaches (Bush et al., 2018; Catalán-Gil et al., 2019; Catalán-Gil et al., 2020; D'Agaro et al., 2020; Gullo et al., 2016). The general conclusion of these investigations is that the application of the DMS cycle to booster systems is as more beneficial as higher the heat rejection temperature (or environment temperature) is. In fact, Catalán-Gil et al. (2019) predicts, for a medium-sized supermarket, annual reductions of electricity consumption between 2.9 to 3.4% in warm regions and from 3.0 to 5.1% in hot zones. In addition, Dai et al. (2019) have also verified from a theoretical approach that the DMS system is also useful to improve the performance of heat pumps for residential heating, with predicted COP increments up to 24.4% (Dai et al., 2020).

The mentioned researches have performed the evaluation of the cycles using pure fluids as refrigerants in the DMS. As Dai et al. (2017) and Nebot-Andrés et al. (2017) point out, the optimum subcooling degree in CO_2 transcritical cycles is relatively high, reaching values as high as 16.5°C (t_o=5°C, t_{env}=30°C). This large subcooling implies a poor temperature match between CO_2 and the refrigerant when a pure fluid is used as refrigerant in the subcooler. It implies the operation at a low evaporation temperature in the DMS cycle and thus a reduction of the overall thermal efficiency of the cycle combination. In an attempt to enhance even more the combination of a DMS and a transcritical CO_2 cycle, Dai et al. (2018) launched a hypothesis about the use of zeotropic refrigerant mixtures with matching glide in the DMS cycle, to reduce the temperature difference in the subcooler and thus to improve the performance of the combination. With a thermodynamic model with pressure dependent overall efficiencies of the compressors and using Refprop 9.1 (Lemmon et al., 2013), they evaluated the performance of zeotropic binary combinations in the DMS. They selected R-32 as based fluid and then evaluated theoretically mixtures with R-290, R-1234yf, R-152a, R-1234ze(E), R-600a and R-1234ze(Z). They determined the optimum working conditions for each refrigerant mixture and concluded that theoretically the COP of a DMS-CO_2 cycle can be improved, and that the optimum heat rejection pressure is further reduced compared to the case of a pure refrigerant. In Dai's study they found that the mixture R-32 with R-152a promised the best results in comparison with the use of R-152a as pure fluid, reaching an increment in COP of about 6.5%. However, Dai's hypothesis has not been verified experimentally for the moment, to the best knowledge of the authors.

Accordingly, this work aims to verify Dai's hypothesis, that is, to corroborate that the use of zeotropic refrigerants in the DMS brings about increments in COP and reductions of heat rejection pressure. This evaluation, to the best knowledge of the authors has not been performed experimentally yet. To accomplish it, first we have adapted Dai's thermodynamic model with the newest version of Refprop 10. (Lemmon et al., 2018) and the experimental efficiency correlations of tested compressors. Then, we have selected the best performing binary mixtures using R-152a as reference fluid. And finally, using an available test bench (Llopis et al., 2016), three zeotropic mixtures have been evaluated in the DMS taking R-152a as reference for three heat rejection levels and one evaporating condition. For the optimum conditions, it has been verified that Dai's hypothesis is true, but that there are different trends that must be considered. Thus, this work discusses the experimental evaluation of Dai's hypothesis, quantifies the improvement, and points out the aspects that must be considered for future implementations of the DMS cycle.

2. Thermodynamic selection of zeotropic blends

2.1. Thermodynamic model

To select the binary mixtures for the experimental evaluation, the thermodynamic model suggested by Dai et al. (2018) has been adapted to the existing experimental plant (Fig. 2). The first modification is the introduction in the model of the overall efficiencies of the compressors, which were obtained from experimental campaigns. Eq. (1) corresponds to the efficiency of the CO_2 compressor (Sánchez et al., 2014) and Eq. (2) to the DMS compressor working

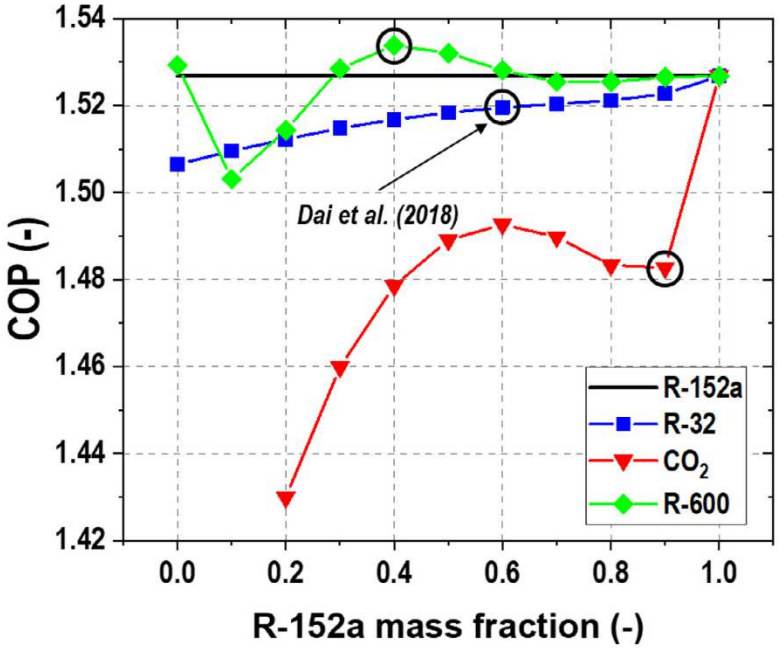

Fig. 1. Optimum theoretical COP at t_o=-14°C and $t_{w,in}$=35°C, as a function of R-152a mass fraction.

with R-1234yf (Llopis et al., 2016).

$$\eta_{G,CO2} = 0.736 - 0.052 \cdot k \quad (1)$$

$$\eta_{G,DMS} = 0.632 - 0.037 \cdot k \quad (2)$$

Then, the simulating conditions were adapted to the known performance of the plant, they being:

- Approach temperature in gas-cooler of 1.5K, since the plant is a water-to-water system.
- Approach temperature in subcooler of 5K.
- Approach temperature in the DMS condenser of 8K.
- DMS condenser subcooling degree of 2K.
- Superheating degree in CO_2 evaporator of 10K and in subcooler of 6K

Finally, using the model, the COP of the CO_2 transcritical cycle with the DMS system (Eq. (3)) was optimized in terms of subcooling degree and heat rejection pressure at a water inlet temperature to the gas-cooler and DMS condenser of 35°C and at an evaporating temperature of -14°C, which were the experimental conditions with the R-152a evaluation (Nebot-Andrés et al., 2021).

$$COP = \frac{\dot{Q}_o}{P_{C,CO2} + P_{C,DMS}} \quad (3)$$

The optimization covered binary mixtures of R-152a with R-32, R-600 and CO_2 in steps of 10% of mass fraction variation. For each fluid and at each operating condition, an optimization to find the best combination of gas-cooler pressure and subcooling degree was performed, with the aim to quantify the best energy efficiency. The COP at such conditions is named 'optimum COP'. Refprop 10 was used to evaluate the thermophysical properties of the fluids (Lemmon et al., 2018).

2.2. Theoretical results

Fig. 1 summarizes the optimum overall COP values with the different evaluated refrigerant mixtures at a water inlet temperature of 35°C and an evaporating level of -14°C. With R-152a the maximum COP reaches 1.527, whereas for the mixtures it varies depending on the R-152a mass fraction. First, it needs to be mentioned that for the existing plant and for the mixture R-152a/R-32 the COP does not present a maximum value, as observed in the theoretical results of Dai et al. (2018); and furthermore, this binary mixture does not overperform the base fluid. Second, the mixture of R-152a/CO_2 presents a maximum value, but lower in terms of efficiency to the base fluid. Finally, the unique binary combination that offers COP improvements in relation to the base fluid is R-600/R-152a, which presents a maximum at 1.534. Thus, at least with one mixture the theoretical model indicates that there is room for improvement.

2.3. Selected refrigerant mixtures

According to the simulations, we decided to test experimentally three binary mixtures in the DMS, whose main characteristics are reflected in Table 1, obtained for a CO_2 evaporation temperature of -14°C, a CO_2 condensing temperature of 50°C, RU = 5K and SUB=2K.

- R-152a: Selected as the reference fluid for the DMS, since it was completely tested in a previous investigation (Nebot-Andrés et al., 2021).
- R-600/R-152a [60/40%]: it was selected from the theoretical simulation (Fig. 1) as the best performing mixture. It was prepared in our lab using n-butane with purity of 99.9% and R-152a at 99.9%, with an uncertainty in the mass composition below 0.1%. This fluid presents lower phase-change temperatures than R-152a, 18% higher specific volume, 14% reduced volumetric cooling capacity, 2% lower COP_{DMS} and a moderate effective glide in the subcooler of 5.1K.
- R-152a/R-32 [60/40%]: Although it does not obtain good theoretical results, it was considered as suggested by Dai et al. (2018), since it was the best proportion for the combination of R-152a and R-32 in their study. Presence of R-32 increases the phase-change temperatures, the suction volume is 31% lower, the COP_{DMS} is similar and it presents 5.9K

Table 1
Selected refrigerants for experimental evaluation and ideal-single-stage cycle performance data of the DMS at t_o=-14°C, t_k=50°C, RU=5K and SUB=2K.

Refrigerant [mass comp.]	M ($g \bullet mol^{-1}$)	$GWP_{5,AR}$ (-)	p_o (bar)	p_k (bar)	v_{suc} ($m \bullet kg^{-1}$)	h_{fg} ($kJ \bullet kg^{-1}$)	VCC_{DMS} ($kJ \bullet m^{-3}$)	COP_{DMS} (-)	$Glide_O$ [K]	$Glide_k$ [K]
R-152a	66.1	137	4.39	11.77	0.075	291.1	3142	7.03	0.0	0.0
R-152a/R-32 [60/40%]	59.6	353	6.97	18.31	0.051	302.9	4776	6.79	5.9	6.5
R-600/R-152a [60/40%]	61.1	55	4.05	10.60	0.089	308.8	2697	6.87	5.1	5.9
R-152a/CO_2 [90/10%]	62.9	123	5.63	15.38	0.062	327.0	4257	7.25	12.3	19.9

effective glide in the evaporator. The mixture was prepared in the lab with a mass uncertainty below 0.1%.

- R-152a/CO_2 [90/10%]: Finally, although not obtaining good results, this mixture was selected to investigate the effect of using a high-effective-glide fluid in the subcooler. Proportion of CO_2 was limited to 10% to be able to operate with the existing plant. In this case, with 12.3K glide in the subcooler, the mixture presents 35% higher volumetric cooling capacity, 3% higher COP_{DMS} and 17% reduced specific suction volume. The mixture was prepared in the lab using CO_2 with 99.9% purity. The uncertainty of the composition is below 0.1%.

Mixture preparation was made in our lab using high purity fluids. Composition uncertainty is below 0.1% in mass.

As mentioned above all the mixtures have been simulated in the theoretical model using Refprop 10 using the standard mixing coefficients, which could lead to uncertainty in evaluating thermophysical properties since they are new defined mixtures. The model, therefore, is not able to supply the necessary accuracy to define the exact behaviour of the mixtures in the system giving rise to the need of an experimental approach.

3. Experimental test bench

3.1. Test bench description

To evaluate the zeotropic binary mixtures a research plant previously built was used (Fig. 2). This plant is composed of a single-stage CO_2 compression cycle, with a double-stage expansion system, that incorporates brazed-plate subcooler (0.576 m^2). Both, back-pressure and expansion valves are electronic and allow controlling the heat rejection pressure and the degree of superheat in the evaporator. The subcooling is provided coupling thermally another single-stage vapour compression system through the subcooler, in which the DMS refrigerant evaporates. This cycle is composed of a semi-hermetic compressor (4.06 $m^3 \bullet h^{-1}$ at 1450 rpm), a shell-and-tube condenser and an electronic expansion valve that is customized for each refrigerant.

Heat dissipation in gas-cooler and DMS condenser is performed with a water loop, allowing the volumetric flow and inlet temperature to be controlled. The heat load is provided with a loop working with a propylene-glycol mixture, also allowing to regulate the volumetric flow and inlet temperature.

The plant is fully instrumented with pressure gauges, thermocouples, Coriolis and volumetric flow meters and digital wattmeters. A complete description of the plant and measurement system is detailed in Nebot-Andrés et al. (2021) work.

3.2. Experimental procedure

The experimental tests were conducted in steady-state conditions according to the following constraints:

- Heat rejection: system was evaluated for all the mixtures at three water dissipation temperatures of 25.1, 30.3 and 35.1°C. This temperature was warranted (±0.2K) at the inlet of the DMS condenser and at the inlet of the gas-cooler (see stars in Fig. 2). The volumetric flow of water was of 1.16 $m^3 \bullet h^{-1}$ at the gas-cooler and of 0.61 $m^3 \bullet h^{-1}$ at the DMS condenser.
- Heat load: the plant was tested only at one evaporating condition, that fixed using an inlet temperature of the glycol-mixture in the evaporator at -1.2°C ± 0.2K, with constant volumetric flow rate of 0.71 ± 0.02 $m^3 \bullet h^{-1}$.
- Heat rejection pressure: it was regulated with the electronic back-pressure using an own PID controller implemented in the monitoring system.
- Subcooling degree: the subcooling degree in the subcooler was regulated with speed variation of the DMS compressor. The CO_2 compressor was always kept at nominal speed (1450rpm).
- Degree of superheat: In the CO_2 evaporator 10K and in subcooler 5K were maintained.

In order to obtain the optimum conditions of the subcooled CO_2 transcritical cycle, the plant was subjected to optimization of heat rejection pressure and subcooling degree with the method proposed by Nebot-Andrés et al. (2020). The optimum COP value was obtained from cooling capacity calculation, Eq. (4), and the direct measurements of compressor power consumption, according to Eq. (3). In Fig. 3, it can be observed the optimization process as function of gas-cooler pressure and subcooling degree (Eq. (5)), where the black points correspond to the experimental measurements. The optimum conditions determination ended when the COP value from a point to another changed less than 1%.

$$\dot{Q}_o = \dot{m}_{CO2} \cdot (h_{O,out} - h_{exp}) \tag{4}$$

$$SUB = t_{sub,in} - t_{sub,out} \tag{5}$$

3.3. Data validation

Considering the calibrated accuracy of the measurement devices, which are described in the work of Nebot-Andrés et al. (2021), the uncertainties of cooling capacity, Eq. (4), and COP, Eq. (3), were evaluated using Moffat's method (Moffat, 1985), reaching maximum uncertainties of 0.84% and 0.95%, respectively. Furthermore, the heat transfer balance in subcooler was considered to check experimentally the consistency of measurements and to contrast that the evaluation of thermodynamic properties of mixtures with Refprop does not introduce large computation errors. Table 2 reflects the percentage deviation between the heat transferred by CO_2 and the mixture in the subcooler, reaching maximum deviations of 3.7%, which are considered good for the purpose of this investigation.

4. Results

Although the experimental campaign covered multiple steady-state conditions for each external condition, at different heat re-

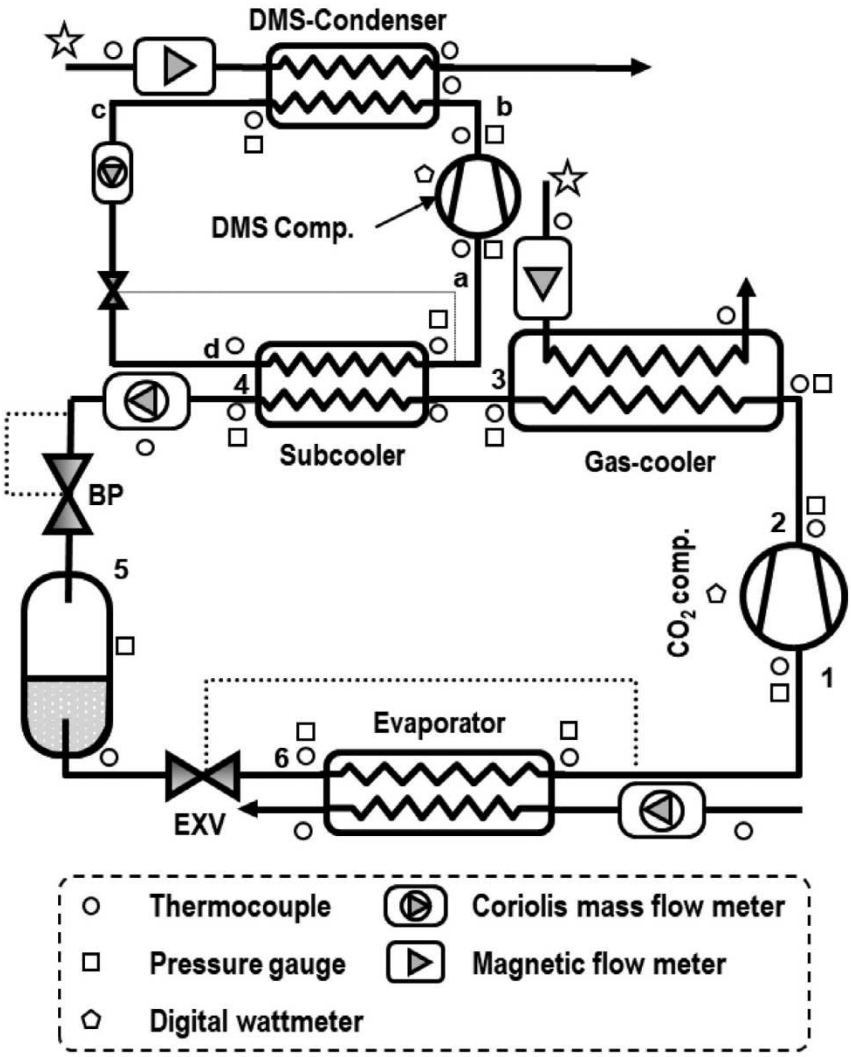

Fig. 2. Scheme of the experimental test bench.

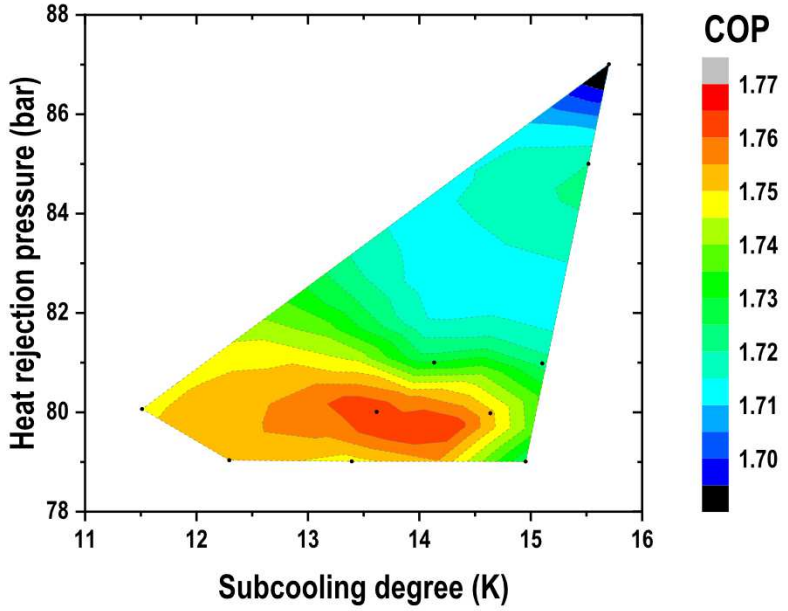

Fig. 3. Experimental optimization of CO_2 – R600/R152a [60/40] at $t_{w,in}$=30.3°C

Table 2
Summary of test conditions, main cycle and DMS cycle indicators at optimum working conditions.

	Test conditions					Cycle indicators				DMS cycle indicators			
	$t_{w,in}$ (°C)	$V_{w,gc,in}$ ($m^3 \bullet h^{-1}$)	$V_{w,DMS,in}$ ($m^3 \bullet h^{-1}$)	$t_{g,in}$ (°C)	$V_{g,in}$ ($m^3 \bullet h^{-1}$)	COP (-)	Q_o (kW)	p_{gc} (bar)	SUB (K)	ε_{sub} (%)	COP_{DMS} (-)	$Q_{o,DMS}$ (kW)	$(Q_{o,DMS} - Q_{SUB})/Q_{SUB}*100$ (%)
R-152a	25.3	1.10	0.62	-1.2	0.70	1.97	7.4	74.9	14.3	87.5	3.98	1.5	-2.6
	30.3	1.15	0.63	-1.1	0.72	1.74	6.9	79.2	14.5	85.7	4.07	1.9	-2.8
	35.0	1.19	0.61	-1.3	0.73	1.53	6.6	90.0	15.3	80.4	3.69	1.8	-3.6
R-152a/R-32 [60/40]	24.9	1.16	0.60	-1.4	0.71	1.88	7.6	74.9	20.0	82.0	2.78	1.9	-1.1
	30.2	1.15	0.62	-1.2	0.71	1.66	7.1	79.9	19.9	83.5	2.71	2.2	-3.5
	35.2	1.15	0.60	-1.3	0.71	1.46	6.7	85.8	21.0	86.0	2.59	2.6	-1.8
R-600/R-152a [60/40]	25.1	1.18	0.61	-1.2	0.72	1.99	7.3	74.9	12.5	75.0	4.65	1.4	-3.2
	30.3	1.16	0.62	-1.2	0.71	1.77	6.9	79.8	13.6	76.0	4.60	1.8	-3.2
	34.9	1.15	0.63	-1.2	0.71	1.55	6.5	89.4	14.2	78.9	4.11	1.7	-2.6
R-152a/CO_2 [90/10]	24.9	1.16	0.60	-1.2	0.71	1.85	7.3	74.9	14.0	60.7	2.53	1.5	-1.9
	30.4	1.16	0.59	-1.3	0.71	1.63	7.0	79.9	15.0	63.7	2.54	1.9	-3.3
	35.2	1.16	0.59	-1.2	0.70	1.41	6.5	87.9	15.5	57.1	2.30	2.0	-3.7

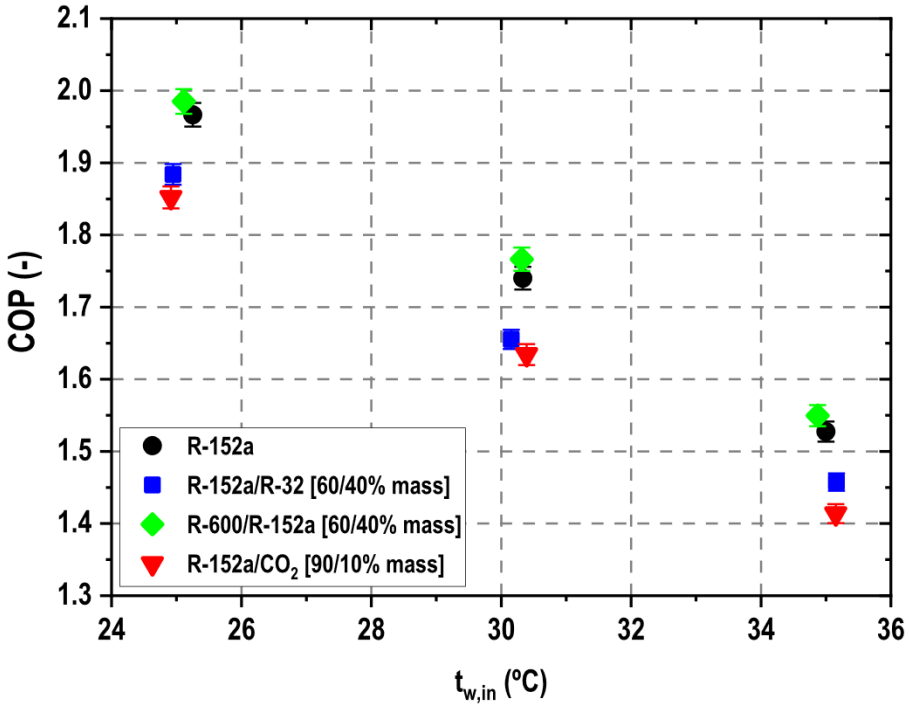

Fig. 4. Optimum experimental COP at $t_{g,in}$ = -1.25°C.

jection pressures and different subcooling degrees, this section focuses only on the optimum conditions.

4.1. Optimum conditions

Optimum conditions, in terms of COP, Eq. (3), for the three heat rejection levels and for the four refrigerants used in the DMS cycle are summarized in Fig. 4. It can be observed that a zeotropic mixture is able to overperform the reference fluid (R-152a). Concretely, the energy improvement achieved by the mixture

R-600/R-152a [60/40] is between 1.1 to 1.4% higher than with R-152a. However, the two other refrigerant blends present COP reductions. R-152a/R-32 [60/40] mixture presents an overall COP decrease between 4.1 to 5% and the R-152a/CO_2 [90/10] mixture a COP cut between 5.6 to 7.9%.

Although the test conditions are different, the measured trends (Fig. 4) coincide with the theoretical simulations summarized in Fig. 1. Thus, it is demonstrated experimentally that it is possible to improve the performance of a dedicated mechanical subcooling system by the use of a zeotropic mixture in the auxiliary cycle, as suggested by Dai et al. (2018).

At optimum conditions (Fig. 4), the partial contribution to the cooling capacity of each refrigeration cycle is presented in Fig. 5, where $\dot{Q}_{sub}$ represents the enhancement of capacity due to the subcooling, Eq. (6), and $\dot{Q}_{base}$ the capacity provided by the CO_2 cycle, Eq. (7).

$$\dot{Q}_{sub} = \dot{m}_{CO2} \cdot \left(h_{sub,out} - h_{gc,out}\right) \tag{6}$$

$$\dot{Q}_{base} = \dot{Q}_O - \dot{Q}_{sub} \tag{7}$$

On the one side, as it can be observed in Fig. 5, the contribution corresponding to the base cycle is similar for each test condition between the different DMS refrigerants. Small variations of this parameter are linked to the different optimum heat rejection pressures, which are lower as higher the subcooling degree is (see Table 2). At reduced heat rejection pressures, the capacity provided by the CO_2 itself is lower. However, large differences are found in the partial contribution to the cooling capacity provided by the subcooler, Eq. (6). For the mixture R-152a/R-32 [60/40] this contribution is between 16.2 and 41.1% higher than with the use of R-152a at optimum conditions, for R-600/R-152a [60/40] ranges between -5.1 to -7.1% and for R-152a/CO_2 [90/10] from 0.4 to 9.1%.

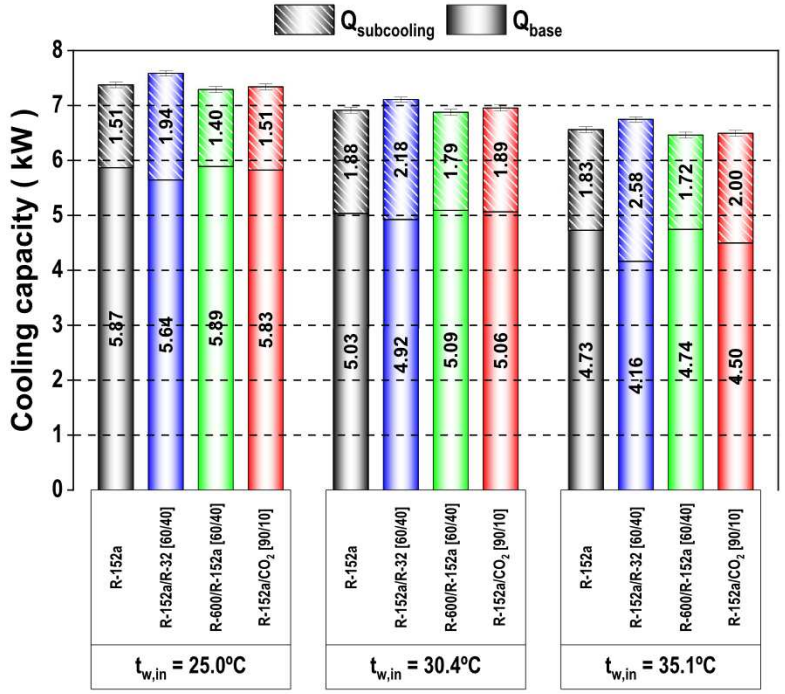

Fig. 5. Cooling capacity at optimum condition at $t_{g,in}$ = -1.25°C.

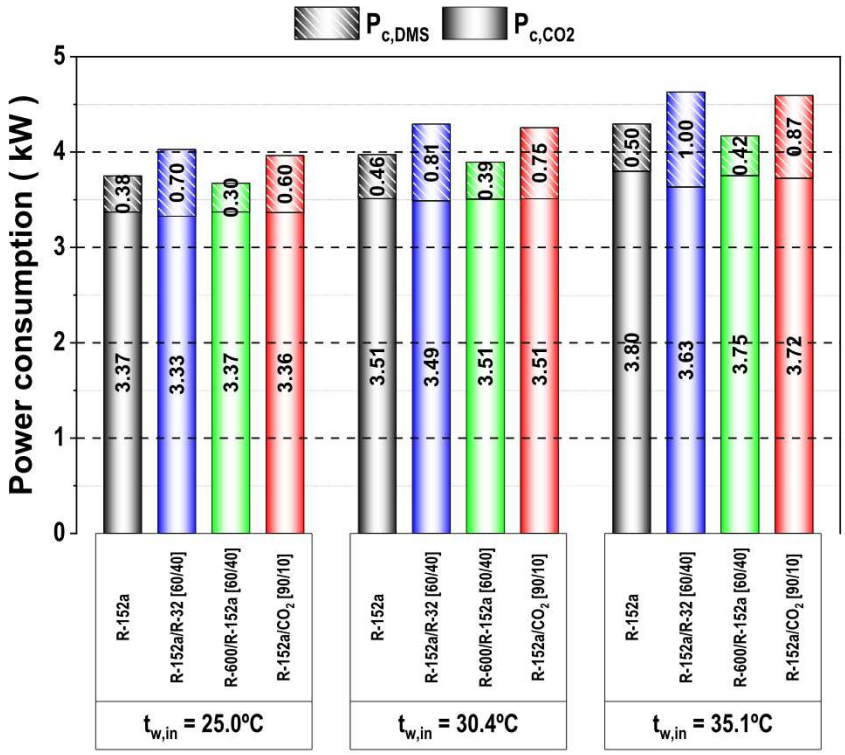

Fig. 6. Power consumption at optimum condition at $t_{g,in}$ = -1.25°C.

These variations are not directly correlated with the VCC_{DMS} parameter (Table 1). Nonetheless, it is important to note that the use of the DMS cycle always intensifies the capacity provided by the cycle.

On the other side, the contribution to the power consumption of each compressor is presented in Fig. 6. It is observed that the power consumption of the CO_2 compressor remains similar between all the refrigerants unlike R-152a/R-32 [60/40] with $t_{w,in}$=35.1°C that, due to the large optimum subcooling degree, allows the CO_2 cycle to work at a lower optimum pressure; on the contrary there are large differences at all conditions with the auxiliary compressor. In this case, refrigerants with high VCC_{DMS} (R-152/R-32 and R-152a/CO_2) show greater cooling capacity and thus have larger power consumption in the DMS compressor. It is worth focusing on the R-600/R-152a [60/40] mixture, that presents a very low power consumption in the DMS compressor, it being between

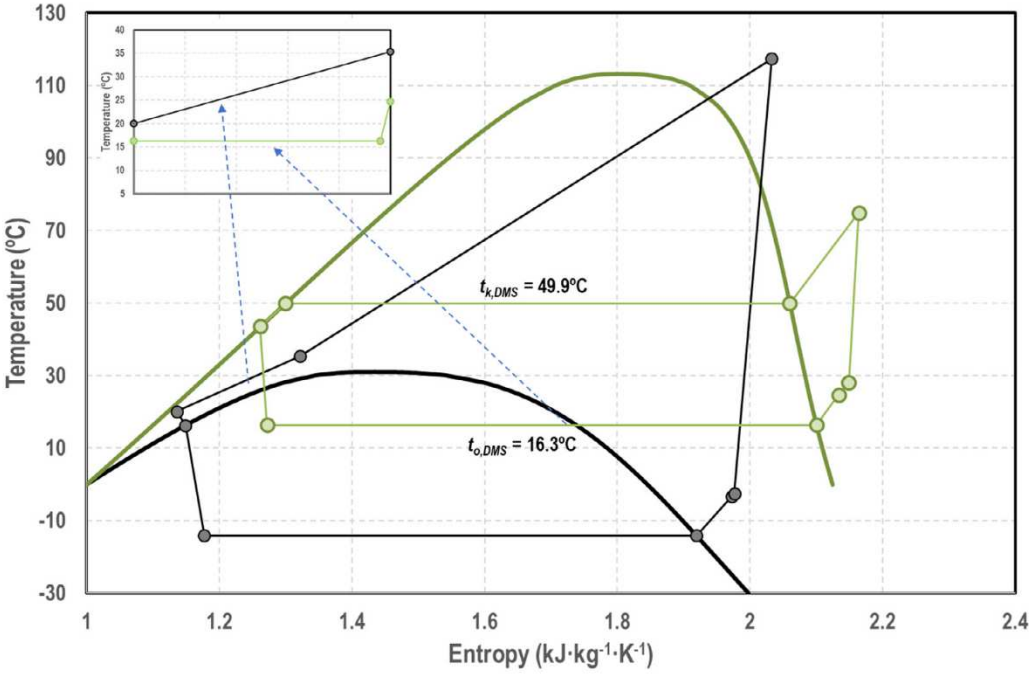

Fig. 7. t-s diagram of CO_2 – R152a at $t_{w,in}$=35.1°C and $t_{g,in}$ =-1.25°C.

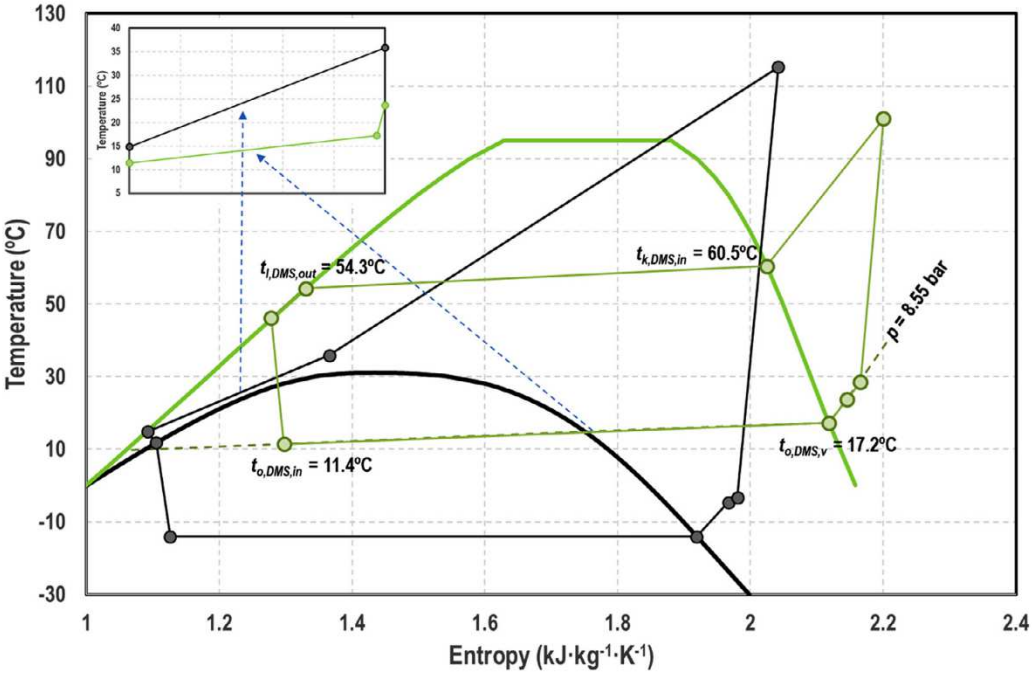

Fig. 8. t-s diagram of CO_2 – R152a/R-32 [60/40] at $t_{w,in}$=35.1°C and $t_{g,in}$ =-1.25°C.

8.9 and 11.2% in relation to the power absorbed by the CO_2 one and between 15.2 and 21.0% lower than that absorbed with the use of R-152a in the DMS cycle. The behaviour of R-600/R-152a [60/40] mixture and thus the optimum conditions when working coupled to the CO_2 cycle are bounded to the high COP_{DMS} values achieved by the mixture (Table 2) which are higher than the values reached with R-152a. Although theoretical COP_{DMS} are higher for R-152a than for R-600/R-152a [60/40] mixture (see Table 1), the experimental COP_{DMS} have an opposite trend, because the working conditions (blend phase-change temperatures) vary, as it is analysed in the following section.

4.2. Operating parameters

As mentioned before, the optimum working condition of the dedicated subcooling cycle, in terms of heat rejection pressure and subcooling degree, is different between the different refrigerant blends. This section analyses closely the working conditions of each combination at dissipation water inlet temperature of 35.1°C.

Figs. 7–10 represent the *t-s* diagram of the different refrigerants, where the estimated temperature profiles in the subcooler are highlighted. For the sake of a graphical representation, they are considered linear without affecting the conclusions of this inves-

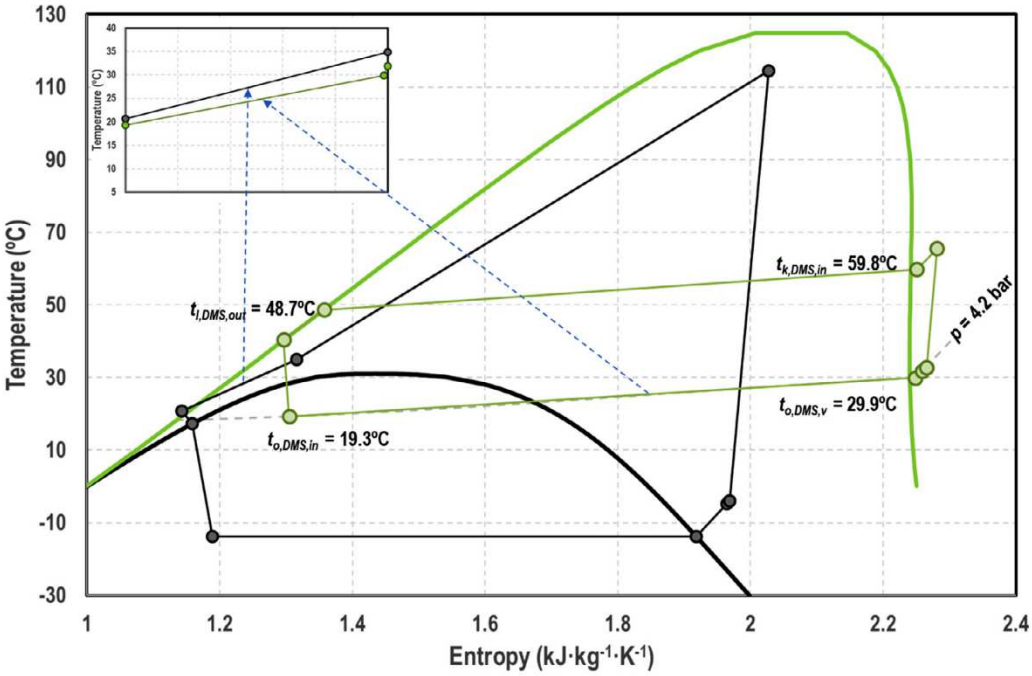

Fig. 9. t-s diagram of CO_2 – R-600/R-152a [60/40] at $t_{w,in}$=35.1°C and $t_{g,in}$ =-1.25°C.

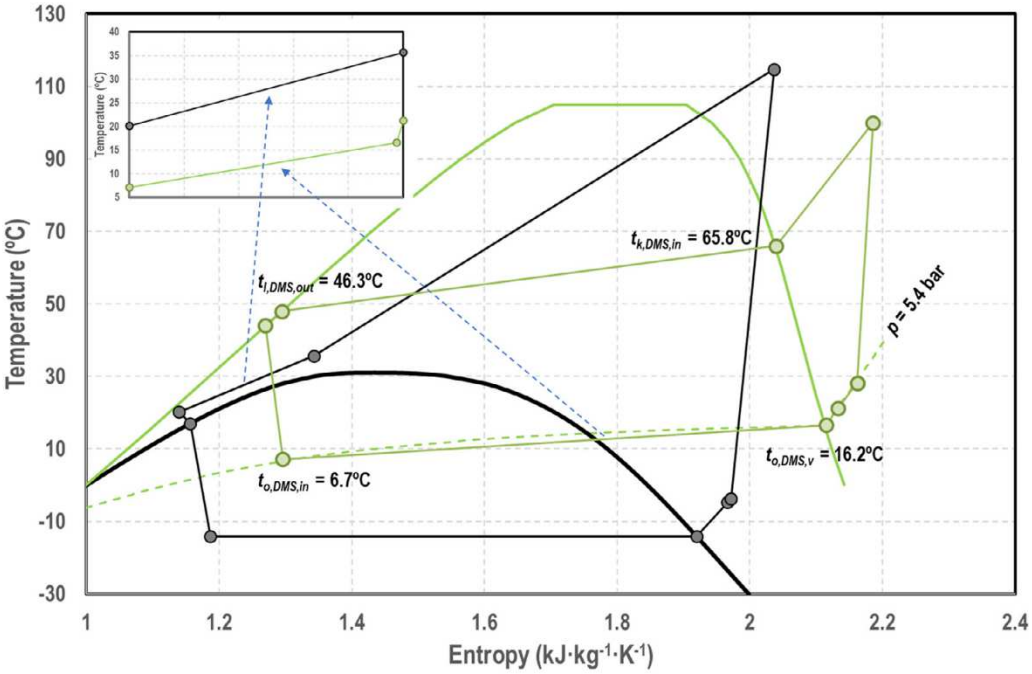

Fig. 10. t-s diagram of CO_2 – R-152a/R-CO_2 [90/10] at $t_{w,in}$=35.1°C and $t_{g,in}$ =-1.25°C.

tigation. Fig. 11 illustrates the phase-change temperatures of the DMS refrigerant. Furthermore, Table 3 summarizes the key parameters of the most representative elements of the plant.

As it can be observed in Figs. 8–10, the use of a zeotropic refrigerant mixture in the DMS cycle introduces a temperature difference through the phase-change temperature. During condensation the temperature decreases, whereas during the evaporation increases. The temperature change or effective glide in the evaporator, Eq. (8), depends upon the components of the blend.

$$Glide_{e,O,DMS} = t_{O,v,DMS,out} - t_{O,DMS,in} \quad (8)$$

Analysing results of Table 3, it is observed that the mixture R-600/R-152a presents the highest effective glide in the subcooler. R152a/CO_2, whose total glide is higher, does not have a large effective glide in the subcooler, since the main change in temperature during the phase-change is produced at lower vapour quality conditions (see isobar in Fig. 10), which are out of the operation of the subcooler.

The best temperature match between R-600/R-152a [60/40] and the CO_2 temperature profile along the subcooler influence the rest of parameters of the subcooler (Table 3). The thermal effectiveness of subcooler, Eq. (9), reaches even higher values than with the use of a pure fluid; the pinch at the exit/inlet of the subcooler,

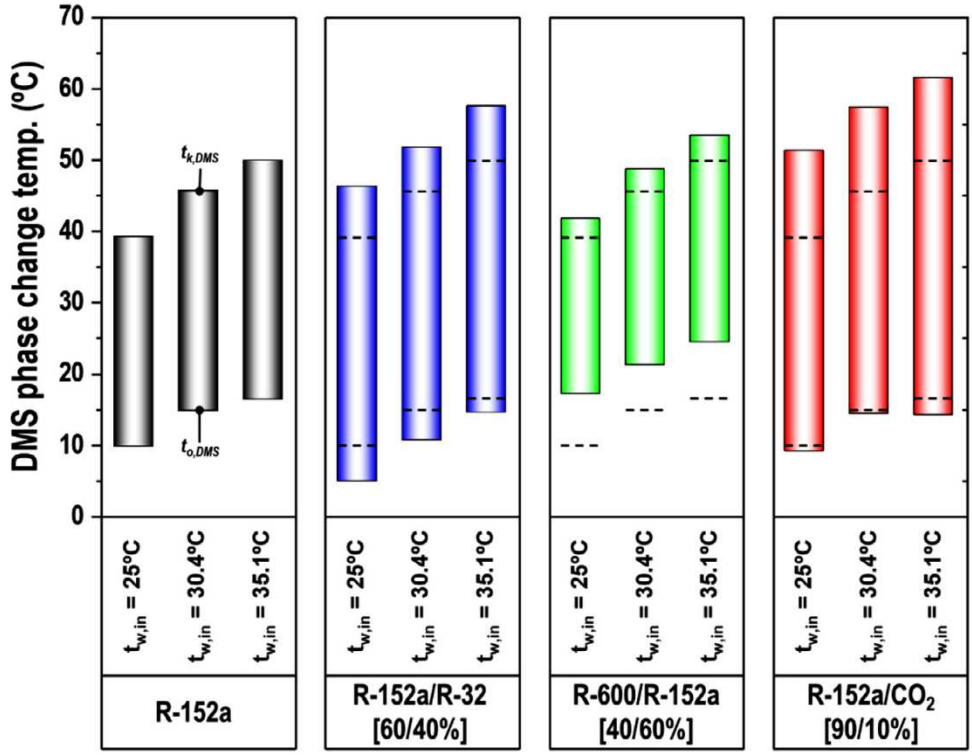

Fig. 11. Phase change temperatures of DMS cycle at optimum conditions at $t_{g,in}$=-1.25°C.

Table 3
Performance operating parameters of key elements at optimum conditions.

	$t_{w,in}$ (°C)	$\eta_{G,CO2}$ (-)	$\eta_{G,DMS}$ (-)	t_{CO2} (-)	t_{DMS} (-)	$Glide_{e,o,DMS}$ (K)	ε_{sub} (%)	Δt_{sub} (K)	Δt_{lmtd} (K)
R-152a	25.3	55.0	43.2	3.3	2.4	-	87.5	2.0	6.8
	30.3	54.2	49.1	3.5	2.5	-	85.7	2.4	7.4
	35.0	53.7	48.5	3.8	2.6	-	80.4	3.7	9.4
R-152a/R-32 [60/40]	24.9	54.5	45.2	3.4	3.4	5.1	67.0	9.9	16.2
	30.2	53.6	45.6	3.5	3.2	5.4	66.6	10.0	16.1
	35.2	53.3	47.9	3.7	3.2	5.6	67.9	9.9	16.5
R-600/R-152a [60/40]	25.1	54.8	30.4	3.3	2.1	10.9	87.5	1.8	2.5
	30.3	54.5	44.8	3.4	2.3	10.7	87.7	1.9	3.2
	34.9	53.5	47.1	3.8	2.3	10.6	91.0	1.4	2.8
R-152a/CO2 [90/10]	24.9	54.6	42.4	3.3	3.6	8.4	61.1	8.9	11.5
	30.4	54.6	47.6	3.5	3.5	8.5	64.1	8.4	11.3
	35.2	53.5	49.4	3.7	3.9	7.8	57.4	11.5	15.0

Eq. (10), reaches lower values than with R-152a; and the logarithmic mean temperature difference, Eq. (11), also reaches lower values than with the reference fluid. For the rest of the blends, which do not have a good temperature match with CO_2, the parameters of the subcooler are worse than with the use of R-152a. Thus, as suggested by Dai et al. (2018), if the refrigerant mixture has a good matching glide with CO_2 temperature profiles, the performance of the system can be improved. It should be noted that the subcooler size was fixed, thus, if the subcooler is resized for each mixture the results could change.

In relation to working temperatures (Fig. 11), it can be observed that for the blends R-152a/R32 and

R-152a/CO_2 the difference between condensation and evaporation temperature increases due to the low thermal performance of the subcooler (Table 3). However, for the mixture R-600/R-152a this difference decreases, and what is more important, the thermal improvement in the subcooler makes the evaporating temperature in the subcooler to be higher and thus, it allows the DMS cycle to work with higher COP_{DMS} values, resulting in a net increment of the COP of the combination, as seen in Fig. 4.

$$\varepsilon_{sub} = \frac{t_{gc,out} - t_{sub,out}}{t_{gc,out} - t_{O,DMS,in}} \tag{9}$$

$$\Delta t_{sub} = t_{DMS,out} - t_{O,DMS,in} \tag{10}$$

$$\Delta t_{lmtd} = \frac{(t_{DMS,out} - t_{O,DMS,in}) - (t_{gc,out} - t_{O,v,DMS,out})}{ln\left(\frac{t_{DMS,out} - t_{O,DMS,in}}{t_{gc,out} - t_{O,v,DMS,out}}\right)} \tag{11}$$

Finally, to illustrate the energy improvement achieved using zeotropic blends in the DMS cycle, irreversibilities in subcooler, Eq. (12) have been evaluated. They are presented in a normalized form in Fig. 12. To normalize the irreversibilities, total exergy destruction in the subcooler has been divided by the cooling capacity of the CO_2 cycle, Eq. (4), and by the death state temperature, which has been considered to be -14°C.

$$\Delta \dot{E}_{X,sub} = t_d \cdot \left[\dot{m}_{CO2} \cdot \left(s_{sub,out} - s_{sub,in}\right) + \dot{m}_{DMS} \cdot \left(s_{DMS,in} - s_{DMS,out}\right)\right] \tag{12}$$

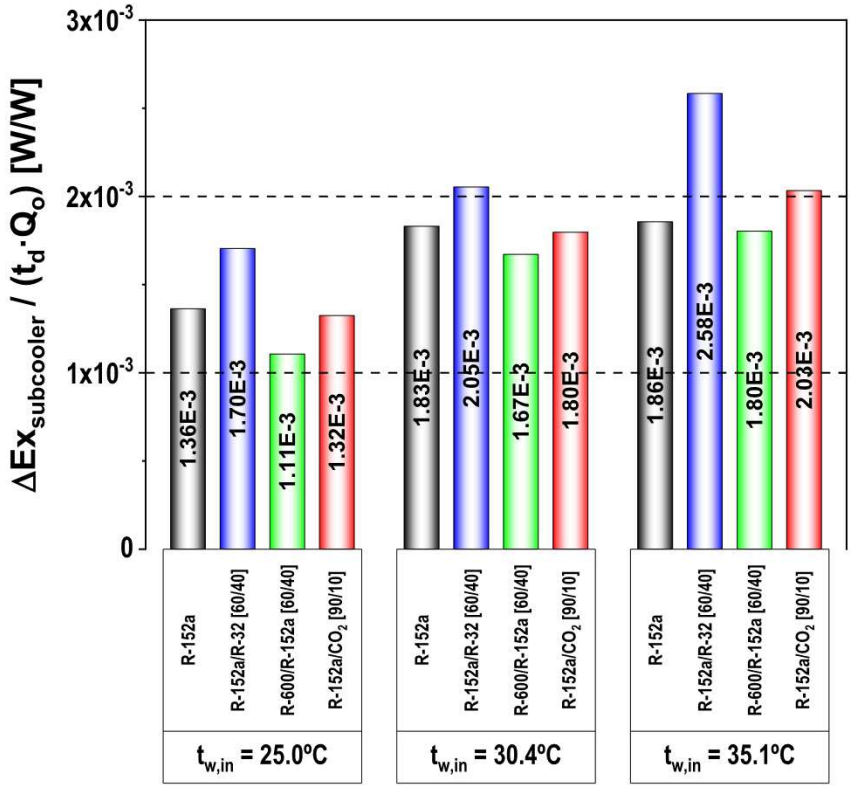

Fig. 12. Normalized exergy destruction in subcooler at $t_{g,in}$=-1.25°C.

Fig. 12 reflects that a good matching glide with CO_2 temperature profile in subcooler allows to reduce the irreversibilities in the subcooler. In this case, the blend R-600/R-152a [60/40] presents a reduction of irreversibilities in relation to R-152a from -2.9 to 18.9%. In addition, also mixture R-152a/CO_2 [90/10] reduces irreversibilities in some operating conditions.

5. Conclusions

In this work the possibility to enhance the performance of a transcritical CO_2 refrigeration plant using a dedicated mechanical subcooling system with zeotropic refrigerant mixtures has been addressed theoretically and experimentally.

Using Dai et al. (2018) model adapted to an existing test plant, the performance of three blends composed of R-32, R-600 or CO_2 with the base fluid R-152a has been evaluated. It has been observed that, theoretically, it is possible obtain higher COP values in relation to the use of pure fluids. However, trends presented by Dai et al. (2018) have not been seen in the simulations. The difference, which cause cannot be defined, could be associated to the different used overall compressor efficiencies and with the update of Refprop, which differ from the previous works. Theoretical simulation has identified the blend R-600/R-152a [60/40%] as the best performing one, with theoretical COP improvements up to 0.46%.

Three refrigerant blends, R-152a/R32 [60/40%], R-600/R-152a [60/40%] and R-152a/CO_2 [90/10%] have been tested experimentally against the operation with R-152a as refrigerant in the dedicated subcooling system. The evaluation was made at fixed conditions of the secondary fluids and covered three heat rejection levels, achieved varying the water inlet temperature to gas-cooler and DMS condenser (25.1, 30.3 and 35.1°C). Experimental campaign has identified the optimum conditions, in terms of subcooling degree and heat rejection pressure, of the plant.

It has been verified that the mixture R-600/R-152a [60/40%] is able to enhance the COP of the plant, with COP increments between 1.1 and 1.4%. In addition, the mixture R-152a/CO_2 [90/10%], which has good matching temperature profiles in the subcooler, could also improve the performance of the plant if the subcooler was resized. However, the other mixtures did not show good performance. The experimental results indicated that the improvements are higher for blends with low volumetric cooling capacity. At optimum conditions, these mixtures work with a moderate subcooling degree and have low power consumption in the auxiliary compressor. Furthermore, as suggested by Dai et al. (2018), the mixtures which effective glide matches with the CO_2 temperature evolution in the subcooler, enhance the thermal performance of the subcooler. Consequently, the evaporating level in the subcooler with the mixture can be higher than with the pure fluid and enhance the performance of the auxiliary cycle and thus of the cycle combination.

Finally, it needs to be mentioned that the use of zeotropic blends in the subcooler allows to reduce the irreversibilities in this heat exchanger, which agrees with Dai's work.

Declaration of Competing Interest

The author declare that they have no known competing financial interests or personal relationships that could have appeared to influence the work reported in this paper

Acknowledgements

Authors gratefully acknowledge the Ministry of Science, Innovation and Universities of Spain (RTI2018-093501-B-C21) and Ministerio de Educación, Cultura y Deporte (Spain) grant FPU16/00151 for financing this research work. The research leading to these re-

sults has also received funding from the MIUR of Italy within the framework of the PRIN2017 project «The energy flexibility of enhanced heat pumps for the next generation of sustainable buildings (FLEXHEAT)», grant 2017KAAECT.

References

Bertelsen, S.K., Haugsdal, S.B., 2015. Design and measurement of a CO2 refrigeration system with integrated propane subcooler at high air temperature operations. Department of Energy and Process Engineering. Norwegian University of Science and Technology, Trondheim, Norway.

Bush, J., Aute, V., Radermacher, R., 2018. Transient simulation of carbon dioxide booster refrigeration system with mechanical subcooler in demand response operation. Sci. Technol. Built Environ. 24, 687–699.

Bush, J., Beshr, M., Aute, V., Radermacher, R., 2017. Experimental evaluation of transcritical CO2 refrigeration with mechanical subcooling. Sci. Technol. Built Environ. 1–13.

Catalán-Gil, J., Llopis, R., Sánchez, D., Nebot-Andrés, L., Cabello, R., 2019. Energy analysis of dedicated and integrated mechanical subcooled CO 2 boosters for supermarket applications. Int. J. Refrig. 101, 11–23.

Catalán-Gil, J., Nebot-Andrés, L., Sánchez, D., Llopis, R., Cabello, R., Calleja-Anta, D., 2020. Improvements in CO2 booster architectures with different economizer arrangements. Energies 13.

Cavallini, A., Cecchinato, L., Corradi, M., Fornasieri, E., Zilio, C., 2005. Two-stage transcritical carbon dioxide cycle optimisation: A theoretical and experimental analysis. Int. J. Refrig. 28, 1274–1283.

D'Agaro, P., Coppola, M.A., Cortella, G., 2020. Effect of dedicated mechanical subcooler size and gas cooler pressure control on transcritical CO2 booster systems. Appl. Therm. Eng., 116145.

Dai, B., Liu, S., Li, H., Sun, Z., Song, M., Yang, Q., Ma, Y., 2018. Energetic performance of transcritical CO 2 refrigeration cycles with mechanical subcooling using zeotropic mixture as refrigerant. Energy 150, 205–221.

Dai, B., Liu, S., Sun, Z., Ma, Y., 2017. Thermodynamic Performance Analysis of CO2 Transcritical Refrigeration Cycle Assisted with Mechanical Subcooling. Energy Procedia 105, 2033–2038.

Dai, B., Qi, H., Liu, S., Ma, M., Zhong, Z., Li, H., Song, M., Sun, Z., 2019. Evaluation of transcritical CO2 heat pump system integrated with mechanical subcooling by utilizing energy, exergy and economic methodologies for residential heating. Energy Convers. Manage. 192, 202–220.

Dai, B., Zhao, X., Liu, S., Yang, Q., Zhong, D., Hao, Y., Hao, Y., 2020. Energetic, exergetic and exergoeconomic assessment of transcritical CO2 reversible system combined with dedicated mechanical subcooling (DMS) for residential heating and cooling. Energy Convers. Manage. 209, 112594.

Gullo, P., Elmegaard, B., Cortella, G., 2016. Energy and environmental performance assessment of R744 booster supermarket refrigeration systems operating in warm climates. Int. J. Refrig. 64, 61–79.

Lemmon, E.W., I.H., B., L., H.M., O., M.M., 2018. NIST Standard Reference Database 23. Reference Fluid Thermodynamic and Transport Properties-REFPROP. National Institute of Standards and Technology Version 10.0.

Lemmon, E.W., Huber, M.L., McLinden, M.O., 2013. REFPROP, NIST Standard Reference Database 23, v.9.1. National Institute of Standards. Gaithersburg, MD, U.S.A.

Llopis, R., Cabello, R., Sánchez, D., Torrella, E., 2015. Energy improvements of CO2 transcritical refrigeration cycles using dedicated mechanical subcooling. Int. J. Refrig. 55, 129–141.

Llopis, R., Nebot-Andrés, L., Cabello, R., Sánchez, D., Catalán-Gil, J., 2016. Experimental evaluation of a CO2 transcritical refrigeration plant with dedicated mechanical subcooling. Int. J. Refrig. 69, 361–368.

Llopis, R., Nebot-Andrés, L., Sánchez, D., Catalán-Gil, J., Cabello, R., 2018. Subcooling methods for CO2 refrigeration cycles: A review. Int. J. Refrig. 93, 85–107.

Moffat, R.J., 1985. Using Uncertainty Analysis in the Planning of an Experiment. J. Fluids Eng. 107, 173–178.

Nebot-Andrés, L., Catalán-Gil, J., Sánchez, D., Calleja-Anta, D., Cabello, R., Llopis, R., 2020. Experimental determination of the optimum working conditions of a transcritical CO2 refrigeration plant with integrated mechanical subcooling. Int. J. Refrig. 113, 266–275.

Nebot-Andrés, L., Llopis, R., Sánchez, D., Catalán-Gil, J., Cabello, R., 2017. CO2 with Mechanical Subcooling vs. CO2 Cascade Cycles for Medium Temperature Commercial Refrigeration Applications Thermodynamic Analysis. Appl. Sci. 7, 955.

Nebot-Andrés, L., Sánchez, D., Calleja-Anta, D., Cabello, R., Llopis, R., 2021. Experimental determination of the optimum working conditions of a commercial transcritical CO2 refrigeration plant with a R-152a dedicated mechanical subcooling. Int. J. Refrig. 121, 258–268.

Park, C., Lee, H., Hwang, Y., Radermacher, R., 2015. Recent advances in vapor compression cycle technologies. Int. J. Refrig. 60, 118–134.

Sánchez, D., Aranguren, P., Casi, A., Llopis, R., Cabello, R., Astrain, D., 2020. Experimental enhancement of a CO2 transcritical refrigerating plant including thermoelectric subcooling. Int. J. Refrig..

Sánchez, D., Patiño, J., Sanz-Kock, C., Llopis, R., Cabello, R., Torrella, E., 2014. Energetic evaluation of a CO2 refrigeration plant working in supercritical and subcritical conditions. Appl. Therm. Eng. 66, 227–238.

Torrella, E., Sánchez, D., Llopis, R., Cabello, R., 2011. Energetic evaluation of an internal heat exchanger in a CO2 transcritical refrigeration plant using experimental data. Int. J. Refrig. 34, 40–49.